Cardiac reversible growth & remodeling model: predicting and understanding the chronic effects of bioinjection therapy

Lik Chuan Lee, Martin Genet, Jonathan Wenk, Joakim Sundnes, Samuel Wall

SB³C2015
Summer Biomechanics, Bioengineering and Biotransport Conference
June 17-20,, 2015, Snowbird Resort, Utah, USA

CARDIAC REVERSIBLE GROWTH & REMODELING MODEL: PREDICTING AND UNDERSTANDING THE CHRONIC EFFECTS OF BIOINJECTION THERAPY

Lik Chuan, Lee
Michigan State University
Lansing, MI, USA
lclee@egr.msu.edu

Martin Genet
ETH Zurich
Zurich, Switzerland

Jonathan Wenk
University of Kentucky
Lexington, KY, USA

Joakim Sundnes
Simula Research Laboratory
Oslo, Norway

Samuel Wall
Simula Research Laboratory
Oslo, Norway

INTRODUCTION

Computational modeling has increasingly been used to elucidate the effects of heart failure (HF) treatments. Most such models are, however, confined to simulating the acute treatment effects, and do not directly simulate the effects of chronic LV remodeling (and reverse remodeling). Since left ventricular (LV) remodeling and reverse remodeling are hallmarks of many cardiac diseases and favorable response to HF treatments, the ability to simulate and predict these chronic effects would have significant impact on the use of computational modeling for patient care. Here, we apply a recently proposed reversible cardiac volumetric growth model [1] to simulate and predict the chronic effects of an emerging bioinjection therapy that is intended to stiffen the infarct [2].

METHODS

Volumetric growth was described by multiplicatively decomposing the deformation gradient $\mathbf{F}$ into a growth component $\mathbf{F}_g$ and an elastic component $\mathbf{F}_e$, i.e.,

$$\mathbf{F} = \mathbf{F}_e \cdot \mathbf{F}_g \,. \tag{1}$$

Growth in the fiber $\mathbf{f}$ direction was described by parameterizing $\mathbf{F}_g$ with a scalar growth multiplier θ (i.e., $\mathbf{F}_g = \theta \mathbf{f} \otimes \mathbf{f}$) that was described using the following constitutive relation [1]. Denoting $\bar{\lambda}_h$ as the average homeostatic elastic myofiber stretch for each cycle, the local evolution of the growth multiplier θ was described by

$$\dot{\theta} = k(\theta)(\bar{\lambda}_e - \bar{\lambda}_h) \,, \tag{2}$$

where $k(\theta) \geq 0$ is a rate limiting function whose main purpose is to ensure that θ lies within some physiological values (i.e, $\theta_{\min} \leq \theta \leq \theta_{\max}$). It has the feature that $k(\theta) \to 0$ as $\theta \to \theta_{\min}$ or $\theta \to \theta_{\max}$. In Eq. (2), growth ($\dot{\theta} > 0$) or shrinkage ($\dot{\theta} < 0$) occurs when the average myofiber stretch $\bar{\lambda}_e$ exceeds or falls below the homeostatic stretch $\bar{\lambda}_h$, respectively.

The growth constitutive model was integrated into a cardiac electromechanics model described by Sundnes et al. [3]. Briefly, cardiac electrophysiology described by the bidomain equations and a cellular electrophysiology model was coupled to a cardiac mechanics model comprising of a Fung-type passive constitutive model and an active stress constitutive model. The elastic deformation gradient tensor $\mathbf{F}_e$ in Eq. (1) enters the Cauchy stress tensor which is given as follows:

$$\boldsymbol{\sigma} = \frac{1}{\det \mathbf{F}_e} \mathbf{F}_e \cdot \frac{dW(\mathbf{E}_e)}{\mathbf{E}_e} \cdot \mathbf{F}_e{}^T + \frac{1}{\det \mathbf{F}_g} \boldsymbol{\sigma}^a(\mathbf{s}, \lambda_e, \dot{\lambda}_e) - p\mathbf{I} \,. \tag{3}$$

In Eq. (3), W is the Fung-type strain energy function, $\mathbf{E}_e = \frac{1}{2}(\mathbf{F}_e{}^T \mathbf{F}_e - \mathbf{I})$ is the elastic Green strain tensor, $\boldsymbol{\sigma}^a$ is the active stress that is a function of (i): state variables $\mathbf{s}$ describing membrane channels and intracellular ionic concentration, and (ii): elastic myofiber stretch λ_e and rate of stretch $\dot{\lambda}_e$. The active stress $\boldsymbol{\sigma}^a$ is scaled by $1/\det \mathbf{F}_g$ to ensure that the active force per unit cell remained constant and does not increase or decrease with cellular growth and shrinkage, respectively.

The coupled growth-electromechanics model was applied to a human LV geometry using standard finite element method with an operator splitting scheme [3]. The epicardial edge of the LV was fixed and pressure was applied to the LV endocardial surfaces. Fiber helix angle with a transmural variation from -60° (endocardium) to 60° (epicardium) was prescribed to the LV [4]. The cardiac cycle was simulated by stimulating the LV at the apex. End-diastolic and aortic valve opening pressures of 13.5 mmHg and 52.5 mmHg were prescribed to the LV model, respectively, and the ejection phase was described using a 3-parameter Windkessel model. Timescale between growth and acute hemo-

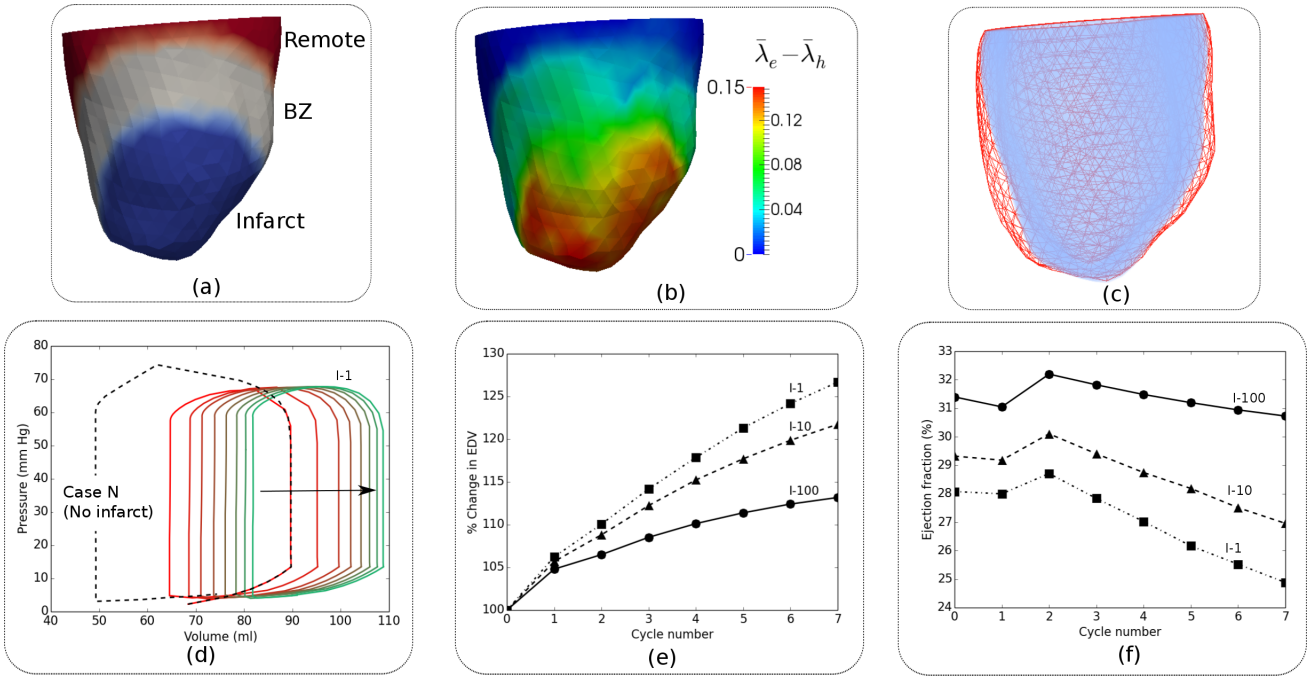

FIGURE 1. (a): Material regions in the LV. (b): Difference between average elastic myofiber stretch and its homeostatic value - driver of the remodeling process (I-1). Note: only BZ and remote regions are allowed to grow. (c): Remodeled LV (red) superimposed onto the original LV (blue) at ED (I-1). (d) Rightward shifting of PV loop during remodeling (I-1). Effects of increasing infarct stiffness on (e): rate of change of EDV and (f): EF.

dynamic loading was separated by locally updating the growth multiplier θ at the end of each cardiac cycle.

Four cases were simulated, namely, LV with homogeneous normal contractility (N), an apical non-contracting and non-growing transmural infarct that was (I-1) unstiffened, (I-10) 10 times stiffer and (I-100) 100 times stiffer. A borderzone (BZ) with half the normal contractile strength was prescribed in the last 3 cases (Fig. 1a). The homeostatic stretch field $\bar{\lambda}_h$ was prescribed using the average elastic myofiber stretch from case N.

RESULTS

In the presence of infarct (I-1, I-10 and I-100), the average cycle myofiber elastic stretch became greater than its homeostatic value at the BZ and infarct (Fig. 1b). As a result, the LV remodeled and became more spherical (Fig. 1c). This result is manifested by a rightward shift of the pressure-volume (PV) loop with both an increase in the end-systolic volume (ESV) and end-diastolic volume (EDV) (Fig. 1d).

With increasing infarct stiffness, however, the rate of increase in ESV and EDV was reduced substantially. A 100-times increase in infarct stiffness led to about a 10 percentage point reduction of the increase in EDV (Fig. 1e) and ESV (not shown) by the 7th growth cycle. Correspondingly, LV ejection fraction (LVEF) was less reduced with stiffer infarct (Fig. 1f). In I-100, LVEF remained fairly constant at about 30%.

DISCUSSION

We have integrated a reversible growth model to a cardiac coupled electromechanics model and have applied it to study the effects of material-induced stiffening therapy by varying the degree of infarct stiffness. Our results suggest that therapeutic benefits in the form of attenuating the remodeling process can be achieved via stiffening the infarct. Specifically, the rate of increase in both EDV and ESV during remodeling were found to be reduced with increasing infarct stiffness. Similarly, our results also indicate that infarct stiffening can attenuate the rate of decrease in EF during remodeling.

These results are consistent with experimental studies using ovine MI model [2]. In that study, transmural infarct was stiffened and thickened by injecting it with a reactive tissue filler agent within hours of coronary occlusion. At 8-week follow up, LV remodeling was found to be attenuated in animals that underwent the therapy when compared to those that did not. The increase in LV volumes were found to be lower in treated animals (ESV : 39% and EDV : 28%) compared to untreated animals (ESV : 83% and EDV : 65%), which is qualitatively consistent with our findings (Fig. 1e). And LVEF was found to decrease at a slower rate in treated animals (from 36% to 31%) compared to untreated animals (from 35% to 28%), which is also qualitatively consistent with our findings (Fig. 1f).

In summary, we have shown that the coupled growth-electromechanics model's prediction of the effects of infarct stiffening is generally consistent with existing experimental results on material-induced infarct stiffening therapy. Future works will include calibration of the model using animal-specific data.

REFERENCES

[1] Lee, LC et al. *Biomech. Model. Mechan.*, 2014 (In press)

[2] Morita, M et al. *Ann. Thorac. Surg.*, 92(2):617–24, 2011.

[3] Sundnes, J et al. *Comput. Methods Biomech. Biomed. Engin.*, 17(6):604–15, 2014.

[4] Streeter, DD et al., *Circ. Res.*, 24(3):339–47, 1969.